CURRENT-VOLTAGE CURVES OF POROUS MEMBRANES IN THE PRESENCE OF PORE-BLOCKING IONS

I. Narrow Pores Containing No More Than One Moving Ion

K. HECKMANN, B. LINDEMANN, *and* J. SCHNAKENBERG

From the Second Department of Physiology, Universität des Saarlandes, Homburg-Saar, West Germany, and the Battelle-Institut e. V., Frankfurt/M, West Germany

ABSTRACT We propose a physical model for voltage-dependent conductance changes of excitable cell membranes. It is based on competition of uni- and bivalent ions for chains of stable sites extending through the membrane. These one-dimensional pathways (pores) have different profiles of chemical potential for the two ionic species so that bivalent ions can block the passage of univalent ions at large membrane potentials. We treat the special case that each pore is either empty or, because of electrostatic repulsion, contains no more than one uni- or bivalent ion at a time. A system of linear differential equations describes the time-dependent probabilities of the various possible pore states. The states are limited by transition rate constants involving the profile of the chemical potential, the membrane voltage, the ionic concentrations in the adjacent baths, and electrostatic interactions between the ions. The steady-state solutions (Kirchhoff-Hill theorem) yield expressions for the relationship between the small signal conductance of univalent ions and the concentration of these ions in the external bathing medium (a saturation curve) and for the ionic currents and the steady-state current-voltage curve (N-shaped). From the latter curve we compute the shift of theshold potential caused by concentration changes of the external bathing medium. The model yields a number of predictions which can be tested experimentally.

1. INTRODUCTION

Much has been speculated about the mechanisms which cause the ionic conductances of biological membranes to change with voltage, a process which is a prerequisite for electrical excitation (e.g., 1–5). Since the molecular structures which form and surround the ion-conducting "channels" within the membranes are still unknown, however, these speculations have not yet led to precise and widely accepted models.

In this situation it may be worthwhile to ask which are the most simple and plausible mechanisms causing voltage-dependent conductance changes of the kind observed with biological membranes. We attempt to describe what we feel is probably

the simplest mechanism of the kind. It does not require moving parts of the membrane structure, nor diffusional rate constants which depend on voltage in an arbitrary way. What is required are merely two ionic species which can compete for sites within ion-conducting pores, and which have different rate constants of diffusion in at least one section of the pore. These constants depend on the local electric field in the well-known exponential fashion. We hope that because of its simplicity our model will be of general interest, even if its construction has been based in part on data of a rather special nature, i.e., data obtained on excitable membranes of amphibian epithelia.

2. EXPERIMENTAL FINDINGS

During recent years it was found that plasma membranes of some epithelia are electrically excitable: while stimulated with a pulse of constant current, they develop a transient deflection of membrane voltage reminiscent of the action potential and the hyperpolarizing response of classically excitable membranes (nerve and muscle). It was realized from the beginning that the "action potential" (spike) of amphibian bladder and skin epithelia is based on a resistance increase-decrease cycle (6), which occurs in a membrane close to or identical with the apical (external) surface of the tissue (6, 7). Soon it was shown that the current-voltage curve of such tissues contained the expected section of negative slope, although this section is separated from the normal resting potential by 200–300 mv (8–12). This explains why large polarizing inward currents have to flow continuously to make the epithelial response possible (6).

The resistance increase associated with the rising phase of the spike appears to proceed much faster (when studied under voltage clamp conditions) than the subsequent decrease (8–10, 13) and, in contrast to the decrease (4, 13, 14), is dependent on the presence of Na^+ (or Li^+) in the external medium. The resistance increase can be made more extensive when the initial membrane resistance is lowered by increasing the resting state Na^+ conductance with vasopressin (8, 9, 13, 15), or less extensive by decreasing the initial Na^+ conductance with amiloride (13). Therefore, the resistance increase of the rising phase is very likely a voltage-dependent cutoff of inward Na^+ current.

Besides Na^+, the presence of external Ca^{2+} ions is essential (6, 14). It was found that the threshold voltage which leads into the negative slope section of the current-voltage curve can be lowered by increasing the Ca^{2+} concentration of the external medium (14). Thus it appears that the Na^+ conductance-voltage curve of the excitable membrane, as in nerve and muscle, is S-shaped and, as in nerve and muscle, can be shifted along the voltage axis by changing the external Ca^{2+} concentration (13). It can be shifted in the opposite direction by an increase in the external Na^+ concentration (14), which could be caused by competition of Na^+ and Ca^{2+} for sites in the Na^+ path across the membrane.

When trying to explain the shift of the Na^+ conductance-voltage curve ($g - V$ curve) by Ca^{2+} in nerve, Frankenhaeuser and Hodgkin have considered the possibility that Ca^{2+} might be able to enter Na^+-specific pores from the outer side of the membrane but unable to leave them by the inner side (16). During resting conditions, the inner side of the membrane is sufficiently negative with respect to the outer side to "bind" Ca^{2+} ions within the Na^+ pores, thus blocking Na^+ flow. Depolarization would release Ca^{2+} from the pores, starting an Na^+ flow which, once a threshold value is reached, would cause further depolarization, leading to the rising phase of the action potential. At high external Ca^{2+} concentrations a greater initial depolarization would be necessary to reach the threshold than at low concentrations, explaining the shift of the $g - V$ curve.

In Frankenhaeuser and Hodgkin's treatment, the only variable connecting depolarization and Ca^{2+} concentration is the electrochemical equilibrium of Ca^{2+} between the pores and the external medium, which determines the fraction of Na^+ pores blocked. (The case of narrow pores where the fraction of pores occupied by Na^+ can influence the fraction occupied by Ca^{2+} was not considered by these authors.) Consequently, there could be no less than a 12.5 mv shift per *e*-fold change of the external Ca^{2+} concentration. Since in nerve a shift of 6–9 mv/*e*-fold concentration change was found, Frankenhaeuser and Hodgkin concluded that their hypothesis would not apply to nerve. In frog skin, an equivalent of 18 mv/*e*-fold change of the external Ca^{2+} concentration has been found (14); this suggests that a simple Ca^{2+} valve model of the type suggested by Frankenhaeuser and Hodgkin seems to be applicable. The only difference from the situation described above for nerve would be that in the skin the rising phase of the spike is caused by a successive blockage of Na pores by Ca^{2+}, which enters the membrane from the outside while the outside becomes more positive.

If Na^+ ions pass the membrane through a finite number of pores, all of which can be blocked by Ca^{2+} ions, then one might be able to find "blockage" of Na^+ flow by Na^+ ions as well (saturation). The phenomenon would require that the entry of Na^+ ions into the pores is not the rate-limiting step for Na^+ transport, and would show up as a saturation of the conductance-concentration curve. This phenomenon can indeed be demonstrated in frog skin (9, 13); Na^+ conductance increases with the external Na^+ concentration as long as concentrations are low, while no further increase of Na^+ conductance with concentration is found when concentrations are high.

In order to compare the Ca^{2+} valve model by Frankenhaeuser and Hodgkin quantitatively with our experimental data on shifts of the $g - V$ curves with the external Ca^{2+} and Na^+ concentrations and saturation of the membrane conductance with increasing Na^+ concentration, we need to compute the fraction of pores occupied by Na^+ and by Ca^{2+} at any membrane voltage and any combination of the external Na^+ and Ca^{2+} concentrations. Knowing these, flows and conductances can be computed as

functions of membrane voltage. Such calculations will be attempted in the following sections.

3. CONSTRUCTION OF THE MODEL

3.1 *Basic Description*

Our model consists of pores which are thought to be one-dimensional paths of stable ionic sites. The paths may be straight or curved; the sites may be separated by distances larger or smaller than the diameters of Na^+ or Ca^{2+} ions. Ions can hop from one site to the next in either direction by overcoming the barrier of chemical potential which separates the two sites. The pores can be entered by Na^+ and Ca^{2+} ions. Therefore, they are characterized by two different profiles of chemical potential, one for Na^+ (Fig. 1 *a*) and one for Ca^{2+} (Fig. 1 *b*), and need not have the same number of sites. One barrier, located near the inner border of the membrane, is extremely high for Ca^{2+} ions (Fig. 1 *b*). (In subsequent calculations, the Ca^{2+} concentration beyond this barrier will mostly be taken to be zero.) This assumption of one large Ca^{2+} barrier will allow the model membrane to behave like a valve: because of their twofold electric charge the Ca^{2+} ions will, particularly at high voltages, be forced into the pores more strongly than the Na^+ ions, block the pores, and suppress Na^+ flow. The electric current (Na^+ flow) will decrease with increasing voltage in the blocking region (negative differential resistance).

Our model is mathematically described by a system of linear differential equations for the time-dependent probabilities of the various possible pore states. If each of the $n - 1$ sites in the pores can be empty or occupied by Na^+ or Ca^{2+}, a pore can exist in

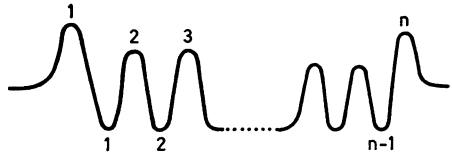

FIGURE 1 *a* Chemical potential of Na^+ ions (the numbers at the minima and at the barriers denote the position in the membrane).

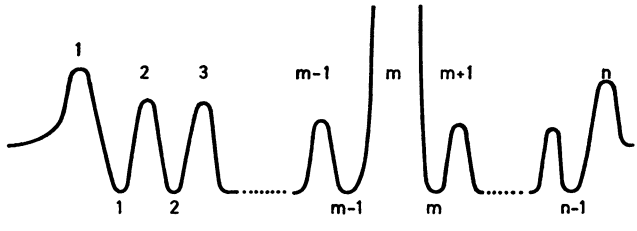

FIGURE 1 *b* Chemical potential of Ca^{2+} ions (blocking barrier at position *m*).

3^{n-1} states. In the system of differential equations, these states are linked by transition rate constants involving the profile of the chemical potential, the membrane voltage, the ionic concentrations in the external medium, and electrostatic interactions between the ions. The steady-state solution can be obtained by setting all time derivatives equal to zero and solving for the steady-state probabilities by matrix inversion.

In the case of $n > 4$ or 5 a mathematical analysis of the complete model is not possible, because of the 3^{n-1} possible states of the pore, and a computer calculation would require too much time; however, numerical solutions and approximate analytic results can be obtained for the two limiting cases: (*a*) pores are empty or contain no more than one ion at a time; (*b*) pores are completelv filled or contain no more than one empty site at a time.

Of these, case *a* is discussed in this paper. It applies to pores free of fixed charges, where states with more than one ion per pore are unlikely for instance because of electrostatic repulsion. To choose an unfavorable situation: if the average distance between two ions in the membrane is $R = 50$ A, the energy of electrostatic repulsion between two ions with valences z_1 and z_2 is given by

$$E = \frac{z_1 z_2 e^2}{4\pi\epsilon_0 \cdot \epsilon \cdot R} = \frac{z_1 z_2 E_0}{\epsilon},$$

where $E_0 \approx 4.6 \cdot 10^{-20} Ws$ and ϵ denotes the mean dielectric constant of the membrane (being about 3 or 4). The rate constants of transition from single to twofold ionic occupation will thus contain a factor

$$\gamma = \exp\left\{-\frac{z_1 z_2 E_0}{\epsilon k T}\right\} \approx \exp\left\{-\frac{10 z_1 z_2}{\epsilon}\right\} \quad \text{for} \quad T = 300°\text{K}.$$

For instance, in the case $\epsilon = 3$ the rate constant k' for transition from a singly occupied pore to a pore occupied by two univalent ions separated by 50 A would be 28 times as small as the rate constant k for the transition from an empty to a singly occupied pore ($\gamma = 0.036$). If one ion were bivalent, k'/k would even be reduced to $(1/28)^2$. Multiple ionic occupation would become still less likely if the critical membrane thickness, i.e. the pore length, were significantly smaller than the total membrane thickness of about 80 A.

3.2 *Derivation of the General Current-Voltage Relation*

Let us denote a state of the membrane pore with Na^+ (Ca^{2+}) at site k by $A_k(B_k)$ and the empty pore by 0. The transition rate constant of Na^+ (Ca^{2+}) is denoted by $a_k(\rightarrow)$ [$b_k(\rightarrow)$] if the ions pass through barrier k of the chemical potential from left to right and by $a_k(\leftarrow)$ [$b_k(\leftarrow)$] if the direction of passage is from right to left. (The

numerical order of sites and barriers is from left to right as indicated in Figs. 1 *a* and *b*.)

Our model may now be represented by the basic diagram of Fig. 2 containing all possible states and all possible transitions between the states. Each line represents two transition rate constants, one for each direction. From this diagram we can easily obtain all differential equations for the probabilities $P(A_k, t)$, $P(B_k, t)$, $P(0, t)$ of the states A_k, B_k, 0; for example,

$$\frac{\mathrm{d}}{\mathrm{d}t} P(A_k, t) = a_k(\rightarrow)P(A_{k-1}, t) + a_{k+1}(\leftarrow)P(A_{k+1}, t) - [a_{k+1}(\rightarrow) + a_k(\leftarrow)]P(A_k, t). \quad (1)$$

The matrix of the rate constants has a very simple structure and thus allows an analytic solution of the steady-state probabilities ($\mathrm{d}P[\cdots]/\mathrm{d}t = 0$) using the normalization condition

$$\sum_{k=1}^{n-1} [P(A_k, t) + P(B_k, t)] + P(0, t) = 1. \quad (2)$$

Since this method is rather tedious, though not difficult, we prefer to apply the theorem of Kirchoff (17), rediscovered by Bott and Mayberry (18), King and Altman (19), and Hill (20). According to this theorem, the Na^+ current per pore is given by the ratio of the sum of the $A(Na^+)$-flux diagrams to the sum of all partia

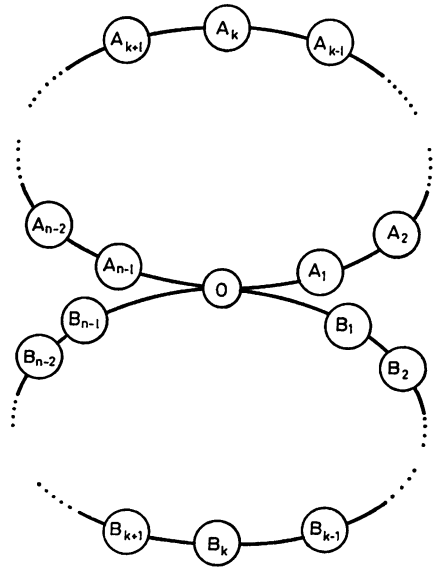

FIGURE 2 Basic diagram of the model.

diagrams[1] of the basic diagram (Fig. 2). For the number of Na^+ ions passing through a part per second we thus obtain

$$j = \frac{\left[\prod_{i=1}^{n} a_i(\rightarrow) - \prod_{i=1}^{n} a_i(\leftarrow)\right] \sum_{j=1}^{n} \beta_j}{\sum_{i=1}^{n}\sum_{j=1}^{n}\left[\alpha_i\beta_j + \sum_{k=1}^{n-1}(\alpha_{ik}\beta_j + \beta_{ik}\alpha_j)\right]}, \tag{3}$$

where

$$\alpha_i = a_1(\leftarrow) \cdots a_{i-1}(\leftarrow)a_{i+1}(\rightarrow) \cdots a_n(\rightarrow), \tag{4}$$

$$\alpha_{ik} = \begin{cases} a_1(\leftarrow) \cdots a_{i-1}(\leftarrow)a_{i+1}(\rightarrow) \cdots a_k(\rightarrow)a_{k+1}(\leftarrow) \cdots a_n(\leftarrow) & i \leq k, \\ a_1(\rightarrow) \cdots a_k(\rightarrow)a_{k+1}(\leftarrow) \cdots a_{i-1}(\leftarrow)a_{i+1}(\rightarrow) \cdots a_n(\rightarrow) & i \geq k+1. \end{cases} \tag{5}$$

$\beta_j\,\beta_{ik}$ are calculated in a similar way. In order to evaluate equation 3 as a function of the external parameters, such as membrane voltage and ionic concentration, we have to determine the various rate constants. Their voltage dependence can be expressed as

$$a_k(\rightarrow) \sim e^{\phi}, \qquad a_k(\leftarrow) \sim e^{-\phi}, \qquad b_k(\rightarrow) \sim e^{2\phi}, \qquad b_k(\leftarrow) \sim e^{-2\phi}, \tag{6}$$

where $\phi = eU/(2nkT)$.[2] Let us assume that all internal Na^+ barriers are equal (in the absence of an external electric field):

$$a_k(\rightarrow) = ae^{\phi}, \qquad a_k(\leftarrow) = ae^{-\phi} \quad \text{for} \quad 2 \leq k \leq n-1; \tag{7}$$

however, before leaving the membrane the Na^+ ion may be confronted with a barrier different from those in the interior:

$$a_1(\leftarrow) = \frac{a}{\kappa}\,e^{-\phi}, \qquad a_n(\rightarrow) = \frac{a}{\kappa'}\,e^{\phi}, \tag{8}$$

where κ, κ' are dimensionless quantities which we expect to be somewhat larger than unity. Local distortions of the internal electric field due to the presence of the charged ions may be neglected in equation 6. Suppose that all pores are occupied by

[1] A partial diagram is obtained from the complete diagram by omitting the minimum possible number of lines such that no cycle is formed. All lines are then directed towards one single point. The numerical value of a partial diagram is the product of the corresponding rate constants. The sum of all partial diagrams is the sum over all ways of forming an undirected partial diagram and over all ways of directing each undirected partial diagram towards one single point. A single A-flux diagram is obtained by omitting the minimum possible number of lines such that only the A cycle is retained. All noncyclic parts of the diagram are directed towards the cycle. The numerical value is the product of the difference between the two cyclic directions and the directed noncyclic part of the diagram. The sum of all A-flux diagrams is the sum over all ways of forming such diagrams.

[2] Only half of the electric potential difference between neighboring sites has to be activated for a hopping transition over the barrier. e = elementary charge, U = membrane voltage, k = Boltzmann's constant, T = temperature.

one univalent ion and that all ions are localized at the same penetration depth (extreme distortion of the field). Treating the ionic layer as a homogeneous layer of electric charge, the discontinuity E of the electric field at the layer is obtained as

$$\Delta E = \frac{q}{\epsilon_0 \cdot \epsilon},$$

where $q = e/F$, and e denotes the elementary charge and F the membrane area per pore. Inserting, for example, a density of 15 pores/square micron and an average dielectric constant of $\epsilon = 4$, we obtain $E = 675$ v/cm. Since the average value of ϵ may well be larger and ions will hardly all be localized in one plane, E will probably be even smaller than estimated here. The estimated value of 675 v/cm has to be compared with the field generated by the applied voltage, which is of the order of 10^4–10^5 v/cm (applied voltage 10–100 mv, membrane thickness 100 A).

The transition rates for entering the membrane are proportional to the ionic concentrations of the external medium, but even when the ionic concentration and the external voltage are disregarded, barriers 1 and n need not be symmetric so that

$$a_1(\rightarrow) = c_A \lambda \frac{a}{\kappa} e^{\phi}, \qquad a_n(\leftarrow) = c'_A \lambda \frac{a}{\kappa'} e^{-\phi}. \tag{9}$$

c_A, c'_A are the Na^+ concentrations at the left and right of the membrane, and λ is a dimensionless factor. Hence, effective concentrations are defined as

$$\bar{c}_A = \lambda c_A, \qquad \bar{c}'_A = \lambda c'_A. \tag{10}$$

The λ factors must be equal on both sides of the membrane since we have to satisfy the equation

$$\frac{c_A}{c'_A} = \frac{\bar{c}_A}{\bar{c}'_A}, \tag{11}$$

which is identical with the condition of microreversibility (i.e., $j = 0$ if $U = 0$ and if $c_A = c'_A$).

Analogous assumptions are made for the Ca^{2+} transition rate constants, except that barrier m is assumed to be extremely high for Ca^{2+} compared with the other internal barriers:

$$b_k(\rightarrow) = be^{2\phi}, \qquad b_k(\leftarrow) = be^{-2\phi} \quad \text{for} \quad 2 \leq k \leq n-1, k \neq m, \tag{12}$$

$$b_m(\rightarrow) = \eta be^{2\phi}, \qquad b_m(\leftarrow) = \eta be^{-2\phi}, \qquad 0 \leq \eta \leq 1. \tag{13}$$

The expressions for $b_1(\rightarrow)$, $b_1(\leftarrow)$, $b_n(\rightarrow)$, and $b_n(\leftarrow)$ are similar to equations 8 and 9.

If we insert the above definitions for the rate constants into equations 3, 4, and 5

we obtain a rather complicated expression for j after some straightforward but lengthy calculation. This expression includes the case of Ca^{2+} overcoming the critical barrier m at very high voltages. Since we do not want to include this case, we simplify our equations by performing the limit $\eta \to 0$, i.e., by making barrier m completely impermeable to Ca^{2+}. In this limit we finally obtain

$$j = a\frac{2c\sinh(\phi) + \Delta c\cdot\coth(n\phi)\cdot\sinh(\phi)}{X_0(\phi)[1 + Y(\phi)] + cX_1(\phi) + \Delta cX_2(\phi)}, \tag{14}$$

where

$$c = \tfrac{1}{2}(c_A + c_A'), \qquad \Delta c = c_A - c_A', \tag{15}$$

and

$$\begin{aligned} X_0(\phi) &= 1 - [\kappa + \kappa' - 2 + (\kappa - \kappa')\coth(n\phi)]\sinh^2(\phi) \\ &\quad + [(\kappa + \kappa' - 2)\coth(n\phi) + \kappa - \kappa']\cosh(\phi)\cdot\sinh(\phi), \end{aligned} \tag{16}$$

$$\begin{aligned} X_1(\phi) &= n - 1 + [(\kappa + \kappa' - 2)\cosh(\phi) - (\kappa - \kappa')\sinh(\phi)] \\ &\quad \cdot(\cosh(\phi) - \coth(n\phi)\cdot\sinh(\phi)), \end{aligned} \tag{17}$$

$$\begin{aligned} X_2(\phi) &= \tfrac{1}{2}\{n\coth(n\phi) - \coth(\phi) - (\kappa - \kappa') \\ &\quad + [\kappa + \kappa' - 2 + (\kappa - \kappa')\coth(n\phi)]\sinh(\phi)\cdot\cosh(\phi) \\ &\quad - [(\kappa + \kappa' - 2)\coth(n\phi) + \kappa - \kappa']\sinh^2(\phi)\}, \end{aligned} \tag{18}$$

$$\begin{aligned} Y(\phi) &= [2\sinh(2\phi)]^{-1}\cdot[c_B(e^{(2m-1)2\phi} - e^{2\phi}) \\ &\quad - c_B'(e^{-(2n-2m+1)2\phi} - e^{-2\phi})], \end{aligned} \tag{19}$$

where c_B, c_B' are the effective Ca^{2+} concentrations analogous to c_A, c_A' but possibly containing a different factor.

This result may be simplified even further if the rate constants for Na^+ desorption in the absence of an external field are assumed to be equal on both sides of the membrane and to coincide with the internal Na^+ rate constants: $\kappa = \kappa' = 1$, see equation 8. In this case we obtain

$$\left.\begin{aligned} X_0(\phi) &= 1, \qquad X_1(\phi) = n - 1, \\ X_2(\phi) &= \tfrac{1}{2}[n\coth(n\phi) - \coth(\phi)]. \end{aligned}\right\} \tag{20}$$

$X_2(\phi)$ in equation 20 is a very smooth function varying from $(n-1)/2$ at $\phi = +\infty$ to 0 at $\phi = 0$ and to $-(n-1)/2$ at $\phi = -\infty$ such that

$$cX_1(\phi) + \Delta cX_2(\phi) \to \begin{cases} (n-1)c_A & \phi \to +\infty \\ (n-1)c & = 0 \\ (n-1)c_A' & \phi \to -\infty \end{cases} \tag{21}$$

$Y(\phi)$, on the other hand, increases very rapidly with increasing ϕ. As $Y(\phi)$ is part of the denominator of j, in equation 14, this increase is the mathematical reason of the negative differential resistance for ϕ or U values in the blocking region.

Compared with the significant increase of $Y(\phi)$, the functions $X_0(\phi)$, $X_1(\phi)$, and $X_2(\phi)$ vary very slowly even in the general case

$$X_0(\phi) \to \begin{cases} \kappa & \phi \to +\infty \\ 1 + \dfrac{\kappa + \kappa' - 2}{n} & \phi = 0 \\ \kappa' & \phi \to -\infty \end{cases} \tag{22}$$

$$X_1(\phi) \to \begin{cases} n - 1 + \kappa' - 1 & \phi \to +\infty \\ (n-1)\left(1 + \dfrac{\kappa + \kappa' - 2}{n}\right) & \phi = 0 \\ n - 1 + \kappa - 1 & \phi \to -\infty \end{cases} \tag{23}$$

$$X_2(\phi) \to \begin{cases} \dfrac{1}{2}(n - 1 + \kappa' - 1) & \phi \to +\infty \\ -\dfrac{1}{2}(\kappa - \kappa')\dfrac{n-1}{n} & \phi = 0 \\ -\dfrac{1}{2}(n - 1 + \kappa - 1) & \phi = -\infty \end{cases} \tag{24}$$

4. MATHEMATICAL DISCUSSION OF THE MODEL

4.1 *The Linear Range of the Current-Voltage Relation*

The electric current j vanishes at

$$\phi_0 = -\frac{1}{2n} \ln \frac{c_A}{c_A'}, \qquad eU_0 = -kT \ln \frac{c_A}{c_A'}. \tag{25}$$

In the vicinity of this point the numerator of equation 14 may be approximated by its first-order expansion term with respect to $U - U_0$

$$j = g(\phi)(U - U_0), \tag{26}$$

where the membrane conductance g as a function of ϕ is given by

$$g(\phi) = \frac{aec}{nkT} \frac{F\left(\dfrac{\Delta c}{2c}\right)}{X_0(\phi)[1 + Y(\phi)] + cX_1(\phi) + \Delta c X_2(\phi)}, \tag{27}$$

with

$$F(x) = \frac{1}{2}\left(x - \frac{1}{x}\right) \ln \frac{1-x}{1+x}. \tag{28}$$

$F(x)$ tends to 1 as $x \to 0$ so that $F(\Delta c/2c)$ may be replaced by 1 for concentration differences which are not too large.

4.2 *Conductance Saturation with Increasing Na^+ Concentration*

In the following we will discuss the Na^+ conductance g, equation 27, as a function of the effective average Na^+ concentration c. Let us assume that ϕ is confined to small values so that $Y(\phi) \leq 1$ (if $\phi \to 0$, $Y(\phi)$ tends to a finite value of the order of n multiplied by the effective Ca^{2+} concentration). Let us further simplify equation 27 by replacing $X_0(\phi)$ by 1, and $X_1(\phi)$ by $n - 1$ (see equation 20) and by neglecting the Na^+ concentration difference Δc. (The following discussion also applies without this simplification, the conclusions being qualitatively the same.)

The Na^+ conductance per pore is now given by

$$g \approx \frac{ae}{nkT} \frac{c}{1 + Y(\phi) + (n-1)c}. \tag{29}$$

Inserting equation 19 and taking the reciprocal of equation 29 we obtain

$$\frac{1}{g} \approx \frac{n}{a}\frac{kT}{e}\left[c_B f(\phi) + n - 1 + \frac{1}{c}\right], \tag{29 a}$$

where

$$f(\phi) = \frac{\exp\left[(2m-1)2\phi\right] - \exp(2\phi)}{2 \sinh(2\phi)},$$

(for $c_B' = 0$). Thus, $1/g$ is linearly dependent on $1/c$ and on c_B. The latter dependence becomes more pronounced when ϕ is increased. Defining the measured small signal conductance per unit membrane area as $G = Ng$, where N is the number of pores per unit area, we may plot $1/G$ vs. c_B and obtain for different membrane potentials straight lines with different slopes. On the ordinate these lines have a common intercept

$$\left(\frac{1}{G}\right)_{c_B=0} = \frac{n}{a}\frac{kT}{Ne}\left(n - 1 + \frac{1}{c}\right), \tag{29 b}$$

which varies linearly with $1/c$. Plotting this intercept vs. $1/c$ will yield another straight line, which intersects the abscissa at $1/c = -(n-1)$. Thus, knowing n, the product $N \cdot a$ can be computed from the slope of the straight line.

With increasing c the conductances g and G will approach plateau values g_s

and G_s:

$$G_s = Ng_s = \frac{e}{kT}\frac{Na}{n(n-1)}, \qquad (29\,c)$$

as indicated in Fig. 3. If n is known from equation 29 b, the measured value of G_s can be used to check the value of $N \cdot a$ computed from equation 29 b.

The rate constant a for Na^+ transitions will be given by

$$a = a_0 \exp\left(-\frac{w}{kT}\right), \qquad (29\,d)$$

where w denotes the energy barrier between adjacent Na^+ sites in the interior of the pore.

Inserting equation 29 d into equation 29 c yields

$$\ln (TG_s) = -\frac{w}{kT} + \text{const.} \qquad (29\,e)$$

This equation may allow the determination of w by measuring G_s as a function of temperature T, provided that temperature-dependent structural changes do not interfere in the range of temperatures used.

Saturation of g with $\bar{c}$ (see equation 29) is only possible if $(n-1)\bar{c}$ can be increased such that it is of the same order as $1 + Y(\phi)$, i.e., if $\bar{c} \geq 1/(n-1)$. Since the thickness of the membrane does not exceed 100 A we expect $n - 1$ to be not larger than 30. This means that the actually observed saturation at 20 mM, i.e. a molar fraction of $4 \cdot 10^{-4}$ (9, 13), implies an effective Na^+ concentration which for $n = 30$ is two orders of magnitude larger than the Na^+ concentration in the solution. This enhancement of the effective concentration can be explained by an effective attraction between the pores and the Na^+ ions. Possible reasons for such an attraction are (a) fixed charges along the pores, or (b) high polarizability of the membrane material.

If, in case a, each pore site is associated with a fixed charge, the most probable pore state would be complete ionic occupation. This situation is the extreme opposite

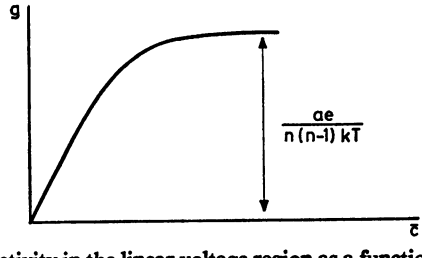

FIGURE 3 Na^+ conductivity in the linear voltage region as a function of the average effective Na^+ concentration $\bar{c}$.

of our model which includes single ionic occupation only (see section 3.1); however, our model will apply to case *a* if only one fixed charge is present, provided that this charge is not localized. Assumption 7 of equal internal Na^+ hopping rate constants (see Fig. 1*a*) will be justified only if the charge is almost uniformly distributed along the pore or even capable of moving within the protein structures forming the pore.

In case *b*, the polarizability of the membrane proteins forming the pore has to be so large that the polarization energy of the Na^+ ion in the pore exceeds its energy of solution. A high polarizability of the membrane material means a high dielectric constant, which in turn considerably reduces the electrostatic repulsion. This would again lead to multiple ionic occupation and thus go beyond the scope of our model, unless the electrostatic repulsion between two ions in the same pore is larger than the effective attraction between the ion and the pore caused by the polarizability of the membrane material.

In either case, *a* or *b*, the observed saturation indicates that the minima of the chemical potential of the Na^+ ions in the pore are lower than their chemical potential in the solution (as indicated in Figs. 1 *a* and 1 *b*).

4.3 *Nonlinear Range: Valve Effect of* Ca^{2+}

From equation 19 we easily obtain

$$Y(\phi = 0) = (m - 1)c_B + (n - m)c'_B \leq 1, \tag{30}$$

whereas for $\phi \to \infty$

$$Y(\phi) \to \tfrac{1}{2}c_B e^{A(m-1)\phi} \gg 1. \tag{31}$$

Comparison of Equations 30 and 31 shows that $Y(\phi)$ increases at values of ϕ greater than a critical value ϕ_s which depends mainly on the magnitude of c_B. If the linear approximation of the numerator of equation 14 is still valid for ϕ_s, we may discuss the behavior of the Na^+ conductance g as a function of ϕ by making again use of equation 29 (neglecting Δc and replacing $X_0(\phi)$ and $X_1(\phi)$ by 1 and $n - 1$, respectively). Confining ourselves to $\phi \geq 0$ we may then expect $g(\phi)$ to change little if $\phi \leq \phi_s$,

$$g(\phi) \approx g_0 = \frac{ae}{nkT} \frac{c}{1 + Y(0) + (n - 1)c}, \qquad 0 \leq \phi < \phi_s, \tag{32}$$

and to decrease rapidly as ϕ approaches and exceeds ϕ_s. Figs. 4 *a* and 4 *b* illustrate these relationships between conductance and voltage and between current and voltage. Let us more precisely define ϕ_s by $g(\phi_s) = g_0/2$ or

$$Y(\phi_s) - 2Y(0) = 1 + (n - 1)c. \tag{33}$$

If Ca^{2+} ions are present only on the outer side of the membrane ($c'_B = 0$), we obtain from equation 33 by inserting equations 19 and 30

$$c_B[f(\phi_s) - 2(m - 1)] = 1 + (n - 1)c, \tag{34}$$

where

$$f(\phi) = \frac{\exp[(2m - 1)2\phi] - \exp(2\phi)}{2 \sinh(2\phi)}. \tag{35}$$

Taking the logarithm of equation 34 yields as an approximation for large values of ϕ

$$\ln c_B + \frac{2m - 1}{n} \frac{eU_s}{kT} = \ln [1 + (n - 1)c], \tag{36}$$

or

$$eU_s \approx -\frac{n}{2m - 1} kT \ln c_B + \text{const.} \tag{37}$$

For small values of ϕ, corresponding to high values of c_B, we have to take account of the detailed structure of $f(\phi)$. This means a positive deviation of the threshold voltage U_s from relation 37.

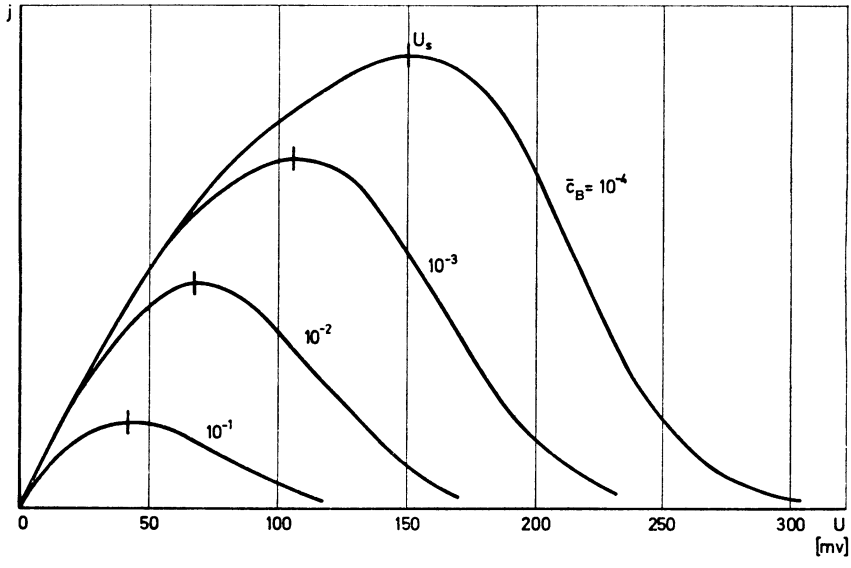

FIGURE 4 *a* Computed curves of Na^+ flux j per pore as a function of membrane voltage U for various values of $\bar{c}_B$ (= external effective Ca^{2+} concentration; internal effective Ca^{2+} concentration $\bar{c}'_B = 0$).

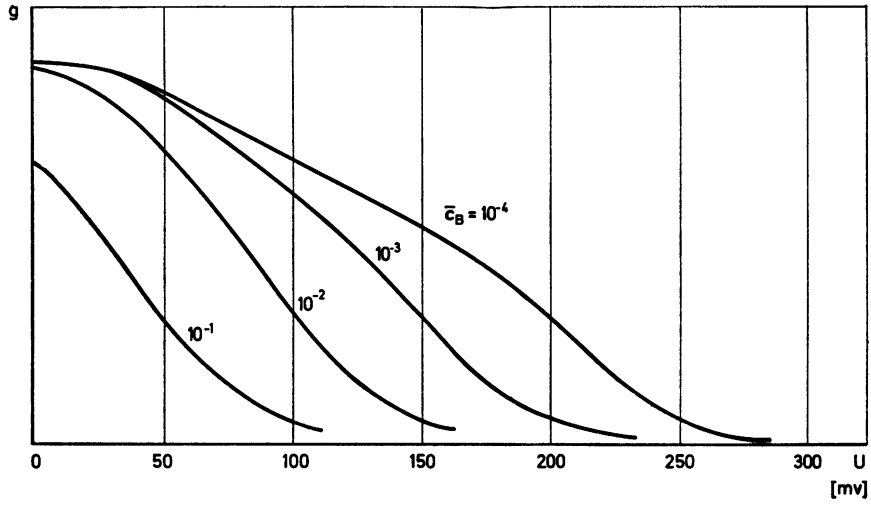

FIGURE 4 *b* Computed curves of Na^+ conductivity g per pore as a function of membrane voltage U for various values of $\bar{c}_B(\bar{c}'_B = 0)$.

The computed curve of eU_s as a function of $\ln \bar{c}_B$ is shown in Fig. 5. The slope of the linear part of this curve is $kTn/(2m - 1)$ and therefore, apart from the factor kT, depends only on the relative position of the Ca^{2+} barrier within the membrane Inserting into equation 37 an experimentally observed value (13, 14) of

$$\frac{d(eU_s)}{kT\, d(\ln \bar{c}_B)} = -0.72 \qquad (\text{for } T = 300°K),$$

we obtain $m/n \approx 0.7$.

As in the treatment by Frankenhaeuser and Hodgkin, we get from equation 37

$$\Gamma_B = \frac{dU_s}{d(\ln \bar{c}_B)} = -\frac{kT}{e}\frac{n}{2m-1} \leq -\frac{kT}{2e} = -12.5 \text{ mv}, \qquad (38)$$

or

$$|\Gamma_B| \geq 12.5 \text{ mv},$$

since $1 \leq m \leq n$. The value of $\Gamma_B = -18$ mv observed in frog skin experiments lies within this range and thus allows the application of our model of singly occupied pores. It should be noted that in all cases where $m/n \neq 0.5$, Γ_B will be different when the electric field is reversed.

In the case of completely occupied pores (each pore site associated with a fixed charge), Heckmann and Vollmerhaus[3] found that the effective equivalence between voltage and concentration may be shifted in favor of the concentration. In this case,

[3] Private communication.

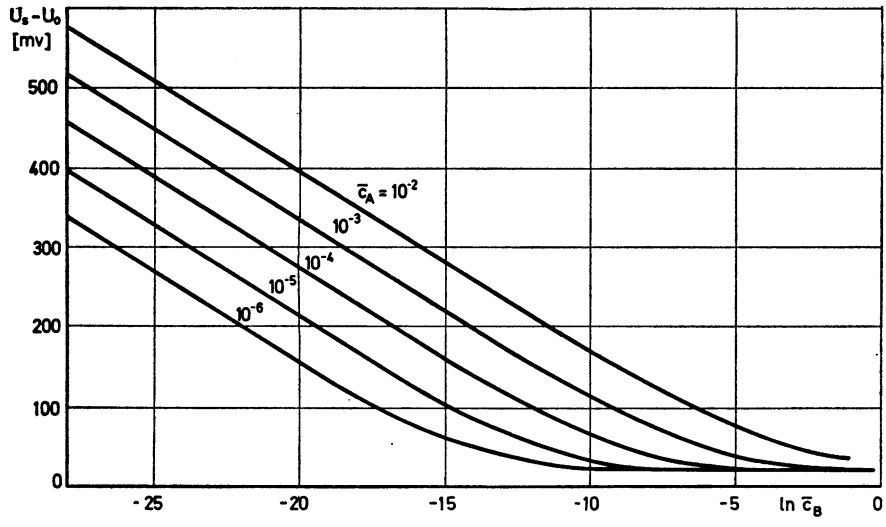

FIGURE 5 Computed curves of $U_s - U_0$ as a function of ln $\bar{c}_B$ (U_s = threshold voltage; U_0 = rest potential). Parameter: external effective Na^+ concentration $\bar{c}_A$; internal effective Na^+ concentration $\bar{c}'_A = 10^{-2}$ (constant for all curves).

a value of $|\Gamma_B| \leq 12.5$ mv may be observed at least in a limited range of the membrane potential.

From equation 34 we may also obtain ϕ_s as a function of the effective average Na^+ concentration c. For large values of c such that $(n-1)\,c \gg 1$ and for large values of ϕ_s we get

$$eU_s \approx \frac{n}{2m-1} kT \ln c + \text{const}, \tag{39}$$

$$\Gamma_A = \frac{dU_s}{d(\ln c)} = \frac{kT}{e} \frac{n}{2m-1}. \tag{39 a}$$

For small values of c and ϕ_s we expect a positive deviation of eU_s from the value given in equation 39. Fig. 6 shows the computed curve of eU_s vs. ln c_A (c'_A being constant) for different Ca^{2+} concentrations c_B.

Let us once more look at equation 34. From equation 35 we derive

$$\lim_{\phi \to 0} [f(\phi) - 2(m-1)] = -(m-1) < 0. \tag{40}$$

Since $f(\phi) \to \infty$ as $\phi \to \infty$, equation 40 implies the existence of a zero $\phi_1 = eU_1/(2n\,kT) > 0$ of $f(\phi) - 2(m-1)$,

$$f(\phi_1) - 2(m-1) = 0, \quad \phi_1 > 0; \tag{41}$$

however, the threshold behavior of the conductance $g(\phi)$ is observed only if the

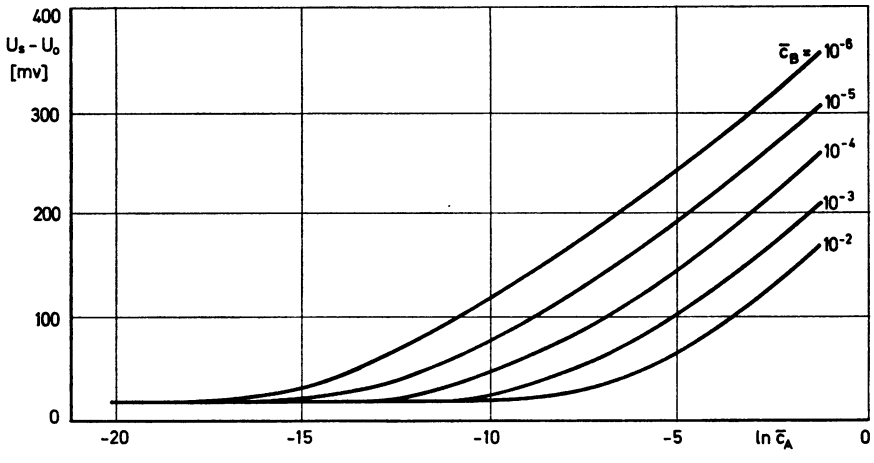

FIGURE 6 Computed curves of $U_s - U_0$ as a function of ln $\bar{c}_A$ for various values of $\bar{c}_B$($\bar{c}'_A = 10^{-2}$, $\bar{c}_B = 0$).

left-hand side of equation 34 is positive and of the order of unity. This means that

$$\phi_s > \phi_1 > 0 \quad \text{or} \quad eU_s > eU_1 > 0$$

for all values of ln c_B as indicated in Fig. 5.

Moreover, for values of ϕ_s near ϕ_0, the factor c_B in equation 34 must be very large since $f(\phi) - 2(m - 1)$ becomes very small. The experimentally observed deviation of eU_s from the linear relation 37 between eU_s and ln c_B therefore implies that the effective Ca^{2+} concentration c_B is much larger than the Ca^{2+} concentration c_B in the solution (0.05–50 mM, i.e., a molar fraction of 10^{-6}–10^{-3}) at least for values of ϕ in the threshold region.

Thus, we have an effective attraction not only between the empty pores and the Na^+ ions, as stated in section 4.2, but also between the empty pores and the Ca^{2+} ions. It seems very likely that the reasons for Ca^{2+} attraction are the same as for Na^+ attraction.

5. GENERAL DISCUSSION

The basic idea of a Ca^{2+} valve mechanism was proposed by Frankenhaeuser and Hodgkin (16). Ca^{2+} can enter Na^+-specific pores from the outer side of the membrane but is unable to leave them by the inner side. When the electric field is increased such that the outer membrane surface becomes more positive in relation to the inner surface, Ca^{2+} is retained more firmly in these pores, blocking Na^+ flow. Thus, the electric field can control the Na^+ current if Ca^{2+} is present. With increasing external Ca^{2+} concentrations, the voltage range where the Na^+ current is effectively modified is shifted in the direction of depolarization, i.e., less voltage is required.

For its application to the electrical excitation of the surface membrane in frog

skin epithelium this concept had to be modified and specified. The observed saturation of small signal conductance with increasing external Na^+ concentration induced the idea of a limited number of narrow Na^+-specific pores across the membrane (9, 13, 14, 21). The pores are assumed to be occupied by no more than one Na^+ or Ca^{2+} ion at a time, i.e., they are relatively empty. Then competition of Na^+ and Ca^{2+} for empty pores must take place so that the number of pores conducting Na^+ is determined by the number of pores blocked by Ca^{2+}, which in turn is dependent on the Na^+ concentration. Thus, the threshold voltage U_s is not only lowered with increasing external Ca^{2+} concentration but also raised with increasing external Na^+ concentration.

Our calculations led to a number of predictions, indicated below, which can be checked experimentally. For frog skin epithelium, the first prediction has already been verified quantitatively, the second one qualitatively.

(*a*) The threshold voltage U_s should decrease with increasing external Ca^{2+} concentrations c_B such that $\Gamma_B = dU_s/d \ln c_B \leq -12.5$ mv at small values of c_B, equation 38.

(*b*) U_s should increase with increasing external Na^+ concentrations such that $\Gamma_A = -\Gamma_B$, equation 39 *a*.

(*c*) At a constant membrane voltage, the reciprocal small signal conductance $1/G$ should be linearly dependent on the external Ca^{2+} concentration c_B. This dependence should become more pronounced when the membrane voltage U is raised, equation 29 *a*.

(*d*) At a constant membrane voltage, $1/G$ should vary linearly with $1/c$, equations 29 *a* and 29 *b*.

(*e*) Since Ca^{2+} ions retained in the pores by high electric fields are assumed to block Na^+ flow, the resistance increase which occurs when U is suddenly raised beyond U_s should proceed faster than the resistance decrease which occurs when U is suddenly dropped below U_s.

It is, of course, an open question, whether and how many of these predictions are compatible with other models. If one prediction is definitely disproved by experiment, our model cannot be used in its present form. If the predictions are fulfilled and the model holds, the observed Γ_B values allow the determination of m/n, the relative position of the high Ca^{2+} barrier in the pore. For instance, $\Gamma_B = -18$ mv means $m/n = 0.7$ (equations 38 and 39). Then, according to equation 37, the U_s value obtained for the outward current should be considerably larger than that obtained for the inward current (Ca^{2+} and Na^+ concentrations being equal on both sides of the membrane). Using equation 29 *b*, we can compute n, the number of sites along a pore, from conductance data. With n and m/n we obtain m, and inserting m into equation 35 yields the function $f(\phi)$. Knowing n, we can also estimate the product $a \cdot N$ from equation 29 *a*. The product of the internal rate constant for Na^+ transition number of pores per square centimeter can also be obtained from equations 29 *b* and 29 *c*. It is not impossible that N can be determined independently by

experiment, for instance by titration using specific inhibitors like amiloride (13). This would provide a value for a (if $a \cdot N$ is known). Furthermore, if w, the energy barrier between adjacent Na^+ sites in the interior of the pore, can be obtained by temperature measurement, a_0 can be computed from equation 29 *d*.

If conductance saturation (Fig. 3) occurs at moderate external Na^+ concentrations, there must be a considerable attraction between pores and Na^+ ions. Furthermore, the decrease of Γ_B at large values of c_B suggests that there must also be an attraction between pores and Ca^{2+} ions. The simultaneous attraction of Na^+ ions and Ca^{2+} ions may be ascribed to a single almost uniformly distributed and possibly mobile negative charge in the "wall" of the pore or to a high polarizability of the membrane material. Both possibilities would favor pores occupied by more than one cation if the pore length is 50 A or larger (see section 3.1); however, the critical pore length or, in more general terms, the critical length of single chains of pore sites need not necessarily be a large fraction of the total membrane thickness of about 80 A. The narrow section of the pore might be less than 20 A in length, leading at both ends into wider sections which communicate with the internal and external aqueous medium. If the ends of the pore are sufficiently wide and filled with electrolyte, the major part of the membrane voltage would drop across the narrow section. If, in addition, the narrow section would extend through a very thin layer of the membrane material, electrostatic repulsion between cations might prevent multiple ionic occupation. Then attraction between cations and empty pores and repulsion between cations and occupied pores would be found, and the two assumptions of (*a*) attraction between pores and cations and (*b*) exclusion of multiple ionic occupation would not be contradictory.

It should be pointed out that the concept of a pore extending through a thin critical layer of the membrane does not mean that n, the number of pore sites, must necessarily be small. If n is found to be large, the sites could be located along an almost straight line but separated by distances which are smaller than the ionic diameters. Alternatively, the distances between sites might be larger than the ionic diameters if the pore has a helical or otherwise curved shape.

This research was partially supported by the Deutsche Forschungsgemeinschaft (SFB 38) and the Battelle Memorial Institute.

Received for publication 12 July 1971.

6. REFERENCES

1. HODGKIN, A. L., and A. F. HUXLEY. 1952. *J. Physiol.* (*London*). **117**:500.
2. MULLINS, L. J. 1960. *J. Gen. Physiol.* **43**(5, Pt. 2):105.
3. LETTVIN, J. Y., W. F. PICKARD, W. S. MCCULLOCH, and W. PITTS. 1964. *Nature* (*London*). **202**: 1338.
4. GOLDMAN, D. E. 1965. *J. Gen. Physiol.* **48**(Suppl.):75.
5. HOYT, R. C. 1963. *Biophys. J.* **3**:399.
6. FINKELSTEIN, A. 1961. *J. Gen. Physiol.* **47**:545.
7. LINDEMANN, B., and U. THORNS. 1967. *Science* (*Washington*). **158**:1473.

8. LINDEMANN, B. 1965. *Biol. Bull.* (*Woods Hole*). **129**(2):391.
9. LINDEMANN, B. 1968. Experimentelle und Theoretische Untersuchungen des Na- und Wassertransportes durch das Epithel der Froschhaut. Habilitationsschrift. University of Saarland, Medical School, Homburg, West Germany.
10. FISHMAN, H. M., and R. I. MACEY. 1969. *Biophys. J.* **9**:127.
11. FISHMAN, H. M., and R. I. MACEY. 1969. *Biophys. J.* **9**:140.
12. FISHMAN, H. M., and R. I. MACEY. 1969. *Biophys. J.* **9**:151.
13. LINDEMANN, B. 1970. *In* Electrophysiology of Epithelia. G. Giebisch, editor. Symposia Medica Hoechst, Reinhartshausen, Schattauer Publishing Company (1971), Stuttgart, West Germany.
14. LINDEMANN, B. 1968. *Biochim. Biophys. Acta* **163**:424.
15. KUTSCHERA, J. 1967. Zur Lokalisierung einer erregbaren Membran im Epithel der Froschhaut. M. D. Thesis. University of Frankfurt, Medical School, Frankfurt, West Germany.
16. FRANKENHAEUSER, B., and A. L. HODGKIN. 1957. *J. Physiol.* (*London*). **137**:218.
17. KIRCHHOFF, G. 1847. *Poggendorffs Ann. Phys. Chem.* **72**(12):495.
18. BOTT, R., and J. P. MAYBERRY. 1954. Matrices and Trees, Economic Activity Analysis. John Wiley & Sons, Inc., New York. 391.
19. KING, E. L., and C. ALTMAN. 1956. *J. Phys. Chem.* **60**:1375.
20. HILL, T. L. 1966. *J. Theor. Biol.* **10**:442.
21. HECKMANN, K., and B. LINDEMANN. 1969. Current-Voltage Curves of Porous Membranes in the Presence of Pore Blocking Ions. Third International Biophysics Congress, Boston.